



University of Guilan

journal homepage: <https://cse.guilan.ac.ir/>

Solving Weakly Singular Fractional Differential Integration Equations Using Multiple Knot B-Splines and Operational Matrices

Ali Jalal Ali ^a, Mostafa Eslami ^{a,*}, Ali Tavakoli ^a^a Department of Applied Mathematics, University of Mazandaran, Babolsar, Iran

ARTICLE INFO

Article history:

Received 15 September 2024

Received in revised form 30 October 2024

Accepted 30 October 2024

Available online 30 October 2024

Keywords:

Error

Polynomial interpolation

Chebyshev nodes

Probability

ABSTRACT

In this article, we propose a new strategy for solving problems associated with weakly singular partial integro-differential equations. Our approach uses Multiple knot B-splines to develop a powerful arithmetical solution. We analyze the functional matrices used in this technique and provide a detailed overview of its functionality. additionally, we demonstrate the convergence of the proposed advance and verify its effectiveness via several numerical simulation.

1. Introduction

In 2020, Dehestani et al. have used collocation approach with Legendre-Laguerre functions to reach an approximate solution to time-integral partial differential equations (FPIDE) whose order is variable and contain weakly singular kernels [1].

Next, in 2021, Sadri et al. Apply the collection method with shifted Chebyshev polynomials of the fifth type to obtain approximate explanations of time-fractional partial integral differential equations with a weak singular kernel [12]. In 2022, Taghipour and Aminikhah have used Pell polynomials with spectral collocation method to derivation of an approximate solution to a fractional integro-differential equation of variable order (FIDE)with weakly singular kernel [14]. In 2023, Ghosh and Mohapatra use the second order system to solve the time class. FPIDE through variable order on a rectangular domain [7]. In this article we deals with the following variable-order fractional integral differential equation with a weak single kernelis considered Ref [14]:

* Corresponding author.

E-mail addresses: mostafa.eslami@umz.ac.ir (M. Eslami)

$${}^c D_0^{\alpha(t)} v(t) = \mu_1 \int_0^t (t-s)^{-\beta} v(s) ds + \mu_2 \int_0^1 k(t,s) v(s) ds + f(t), \quad 0 \leq t \leq 1, \quad (1)$$

with basic conditions

$$v(0) = 0, \quad (2)$$

Wherever μ_1, μ_2 are real numbers, $\beta \in (0,1)$, $k(\cdot, \cdot)$ and f functions are given. In addition, also u is unknown function to be defined, and ${}^c D_0^{\alpha(t)}$ is the fractional Caputo derivative with variable

order α in which $0 \leq \alpha(t) \leq 1$ and for a suitably smooth function $v(t)$ on $(0,1)$, it is defined by [15]:

$${}^c D_0^{\alpha(t)} v(t) = \frac{1}{\Gamma(1-\alpha(t))} \int_0^t \frac{v'(x)}{(t-x)^\alpha} dx \quad (3)$$

Where Γ is the gamma function.

2. Multiple knot B-spline

A polynomial B-spline is a type of B-spline multiple knot that has repeated knot values in its knot vector. A B-spline is a piecewise-defined polynomial used in approximation and interpolation, and is defined by its degree, control points, and knot vector (a series of parameter values that specify where and how the control points affect the curve). When a knot value appears multiple times (known as a multiple knot), it influences the smoothness of the B-spline curve at that point. Key aspects of multiple knot B-spline included as follows [5]. **(a)** the smoothness of the curve decreases at a multiple knot. For example, at a simple knot (one occurrence), the curve is smooth up to the degree minus one derivatives. since the multiplicity of the knot increases, the continuity at the point decreases. If the knot has multiplicity 1, the curve

is continuous along C^{k-1} (smooth up to the $k-1$ -th derivative). If the knot has multiplicity 2. The curve is continuous along C^{k-2} , and so on. Moreover, at maximum multiplicity (equal to the degree of the B-splines), the curve will have a discontinuity at the knot [13]. **(b)** B-spline are known of their local control properties. Multiple knot restricted the influence of control points, given the designer finer control over the curve shape near the knot.

(c) A multiple knot can introduce shape features corners or cups at specific point on the curve, depending on the multiplicity and the arrangement of control points.

In practical applications like computer graphics, CAD, and numerical analysis, multiple knot B-spline provide flexibility to create both smooth and sharp features on curves and surfaces by carefully controlling the multiplicity of knots.

Definition 1. Consider an increasing sequence of knot vectors $E = \{t_i \leq t_{i+1} \leq \dots \leq t_{i+m}, i \in z\}$. When $m \geq 2$ for every $t \in R$, the basis function of the B-spline for the the i-th multiple knot of order m (degree m-1) is obtained as follows:

$$B_{i,m,E}(t) = \begin{cases} 0, & t_i = t_{i+m-1} = t_{i+m}, \\ \frac{t - t_i}{t_{i+m-1} - t_i} B_{i, m-1,E}(t), & t_i < t_{i+m-1}, t_{i+1} = t_{i+m}, \\ \frac{t_{i+m} - t}{t_{i+m} - t_i + 1} B_{i, m-1,E}(t), & t_i = t_{i+m-1}, t_{i+1} < t_{i+m}, \\ \frac{t - t_i}{t_{i+m-1} - t_i} B_{i, m-1, E(t)} + \frac{t_{i+m} - t}{t_{i+m-1} + t_i} B_{i, m-1, E(t)}, & t_i = t_{i+m-1}, t_{i+1} < t_{i+m}. \end{cases} \tag{4}$$

Where

$$B_{i, 1,E}(t) = \begin{cases} 1, & t_i \leq t < t_{i+1}, \\ 0, & otherwise. \end{cases} \tag{5}$$

Figure 1 and Figure 2 show the multiple knot B-spline basis functions of order 2 and degree 1, and order 3 degree 2 for the knot vector $E = [0, 0, 0, 1, 2, 2, 3, 4, 5, 5, 5,]$.

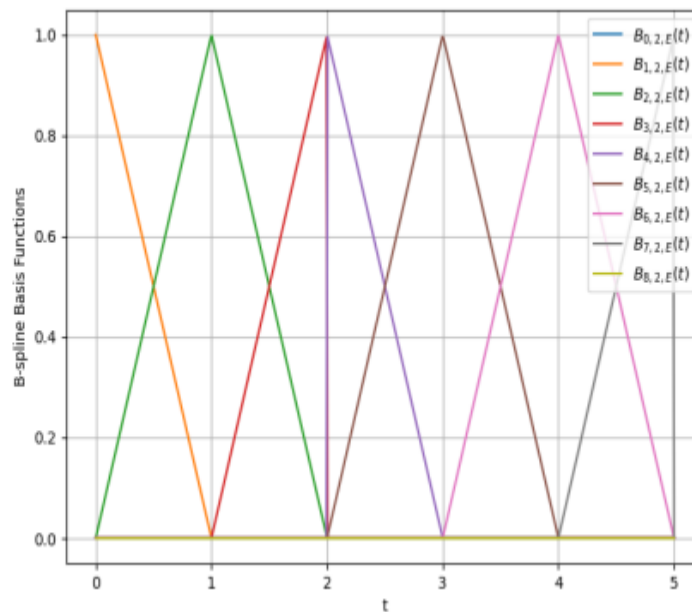


Figure 1. Multiple knot B-spline of degree 1 for note vector E =[0, 0, 0, 1, 2, 2, 3, 4, 5, 5, 5]

Defining the function H by

$$H_{(t)} = \begin{cases} \frac{1}{t}, & t \neq 0 \\ 0, & t = 0. \end{cases} \tag{6}$$

The b-spline of order m for $t_i < t < t_{i+m}$ can be defined as follows:

$$B_{i,m,E}(t) = (t - t_i) H(t_{i+m-1} - t) B_{i,m-1,E}(t) + (t_{i+m-1} - t) H(t_{i+m} - t_{i+1}) B_{i+1,m-1,E}(t) \quad (7)$$

Accordingly, the B-spline of order 2 is defined by

$$B_{i,2,E}(t) = \begin{cases} (t - t_i)H(t_{i+1} - t), & t_i \leq t < t_{i+1} \\ (t_{i+2} - t)H(t_{i+2} - t_{i+1}), & t_{i+1} \leq t < t_{i+2}, \\ 0, & \text{otherwise.} \end{cases} \quad (8)$$

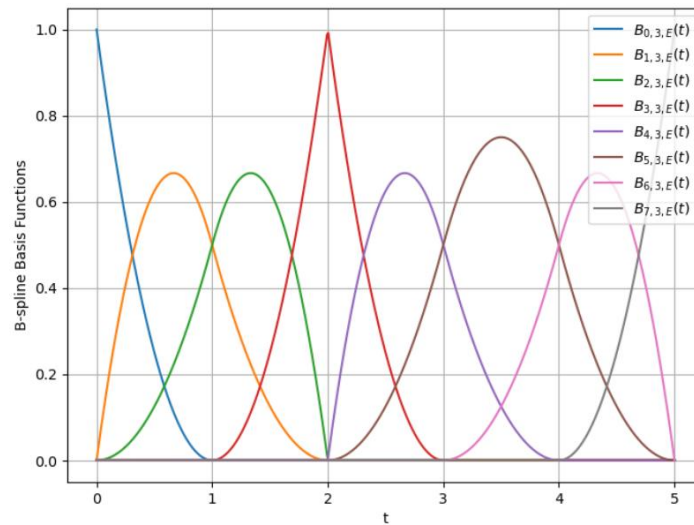


Figure 2. Multiple knot B-spline of degree 2 for knot vector $E = [0, 0, 0, 1, 2, 2, 3, 4, 5, 5, 5]$

For $N \in \mathbb{N}$ and defining

$$\varphi_i(t) = \begin{cases} H(t_{i+1} - t), & t_i < t < t_{i+1}, \\ -H(t_{i+2} - t_{i+1}), & t_{i+1} < t < t_{i+2}, \\ 0 & \text{otherwise.} \end{cases} \quad (9)$$

3. Operational Matrices

In this section, we present the operation matrices obtained from solving problem (1.2) using a Multiple-knot B-spline for this purpose, let u be the solution of Eq. (1) with the initial value of Eq. (2). In this paper, we wish to approximate u in the space covered by the Multiple-knot B-splines method.

$$V = \text{Span}\{\varphi_0, \varphi_1, \dots, \varphi_N\}, \quad (10)$$

On the sequence of knot vectors E , where $\varphi_i = B_{i,2,E}$. Note that because of the initial condition (2), we do not need to add φ_{-1} to V . Let \tilde{v} be a function in the space V . Therefore, we can write

$$v^{\sim}(t) = \sum_{i=0}^N c_i \varphi_i(t). \tag{11}$$

We would like to find the appropriate choice $C = [c_0, c_1, \dots, c_N]^T$ such that $v^{\sim}(t)$ is the best approximate solution to problem (1) - (2) in space V .

Taking $\Phi(t) = [\varphi_{0,J}(t), \varphi_{1,J}(t), \dots, \varphi_{N,J}(t)]^T$ Eq. (11) can be written as

$$\tilde{v}(t) = C^T \Phi(t). \tag{12}$$

Also, for $t_j \leq t \leq t_{j+1}$, we have

$$\begin{aligned} {}^c D_0^{\alpha(t)} v^{\sim}(t) &= \sum_{i=0}^N c_i^c D_0^{\alpha(t)} \varphi_i(t) = \sum_{i=0}^N c_i \int_0^t \frac{d}{dx} \varphi_i(x) \frac{dx}{(t-x)^\alpha} \\ &= c_0 \left[H(t_1 - t_0) \int_0^{t_1} \frac{dx}{(t-x)^\alpha} + H(t_2 - t_1) \int_{t_1}^{t_2} \frac{-dx}{(t-x)^\alpha} \right] + \dots \\ &+ c_{j-1} \left[H(t_j - t_{j-1}) \int_{t_{j-1}}^{t_j} \frac{dx}{(t-x)^\alpha} + H(t_{j+1} - t_j) \int_{t_j}^t \frac{-dx}{(t-x)^\alpha} \right] + c_j H(t_{j+1} \\ &- t_j) \int_{t_j}^t \frac{dx}{(t-x)^\alpha}. \end{aligned} \tag{13}$$

So,

$$\begin{aligned} {}^c D_0^{\alpha(t)} v^{\sim}(t) &= \frac{1}{1-\alpha} \{ c_0 [H(t_1)(-t^{1-\alpha} + (t-t_1)^{1-\alpha}) - H(t_2-t_1)((t-t_1)^{1-\alpha} - (t-t_2)^{1-\alpha})] \\ &+ \dots \\ &+ c_{j-2} [H(t_{j-1}-t_{j-2})(-(t-t_{j-2})^{1-\alpha} + (t-t_{j-1})^{1-\alpha}) \\ &- H(t_j-t_{j-1})((t-t_j)^{1-\alpha} - (t-t_{j-1})^{1-\alpha})] \\ &+ c_{j-1} [H(t_j-t_{j-1})(-(t-t_{j-1})^{1-\alpha} + (t-t_j)^{1-\alpha}) + H(t_{j+1}-t_j)(t-t_j)^{1-\alpha}] \\ &- c_j H(t_{j+1}-t_j)(t-t_j)^{1-\alpha} \}. \end{aligned} \tag{14}$$

This can rewritten as

$$\begin{aligned} {}^c D_0^{\alpha(t)} &= \frac{1}{1-\alpha} \left\{ \sum_{i=0}^{j-2} c_i [H(t_{i+1}-t_i)(t-t_{i+1})^{1-\alpha} - (t-t_i)^{1-\alpha} \right. \\ &- H(t_{i+2}-t_{i+1})((t-t_{i+2})^{1-\alpha} - (t-t_{i+1})^{1-\alpha})] \\ &+ c_{j-1} [H(t_j-t_{j-1})((t-t_j)^{1-\alpha} - (t-t_{j-1})^{1-\alpha}) + H(t_{j+1}-t_j)(t \\ &- t_j)^{1-\alpha}] - c_j H(t_{j+1}-t_j)(t-t_j)^{1-\alpha} \} = C^T D_\Phi^J(t) \end{aligned} \tag{15}$$

where

$$D_{\Phi}^j(t) = [D_0^j(t), D_1^j(t), \dots, D_N^j(t)]^T, \quad (16)$$

and

$$D_i^j(t) = \frac{1}{1-\alpha} \begin{cases} H(t_{i+1} - t_i)(-(t - t_i)^{1-\alpha} + (t - t_{i+1})^{1-\alpha}) \\ -H(t_{i+2} - t_{i+1})((t - t_{i+2})^{1-\alpha} - (t - t_{i+1})^{1-\alpha}), & i = 0, 1, \dots, j-2, \\ H(t_i - t_{i-1})(-(t - t_{i-1})^{1-\alpha} + (t - t_i)^{1-\alpha}) + \\ H(t_{i+1} - t_i)(t - t_i)^{1-\alpha}, & i = j-1, \\ H(t_{i+1} - t_i)(t - t_i)^{1-\alpha}, & i = j, \\ 0, & \text{Otherwis.} \end{cases} \quad (17)$$

The general structure of the matrix

$$D_{\Phi} = [D_{\Phi}^0, D_{\Phi}^1, \dots, D_{\Phi}^N]^T, \quad (18)$$

is as follows:

$$D_{\Phi} = \begin{bmatrix} a & 0 & 0 & \dots & 0 \\ b & a & 0 & \dots & 0 \\ c & b & c & \dots & 0 \\ \vdots & \vdots & \vdots & \ddots & \vdots \\ \dots & \dots & \dots & cb & a \end{bmatrix} \quad (19)$$

where a, b, c are constants. The initial integral in (3.1) can be approximated as follows:

$$\int_0^t (t-s)^{-\beta} v(s) ds \approx \int_0^t (t-s)^{-\beta} v^{\sim}(s) ds = \sum_{i=0}^N c_i \int_0^t (t-s)^{-\beta} \varphi_{i,j}(s) ds, \quad (20)$$

that can be written in compressed form by

$$\int_0^t (t-s)^{-\beta} v(s) ds \approx C^T \Psi^j(t), t_j \leq t < t_{j+1}, \quad (21)$$

where

$$\Psi^j = [\Psi_0^j, \Psi_1^j, \dots, \Psi_N^j]^T, \quad (22)$$

With $\Psi_i^j(t) = \int_0^t (t-s)^{-\beta} \varphi_{i,j}(s) ds$ for $i = 0, 1, \dots, N$ also $t_j \leq t < t_{j+1}$. It should be noted that the matrix formation $\Psi = [\Psi^0, \Psi^1, \dots, \Psi^N]$, and D_{Φ} are the same.

Now, let us discuss the third part of **Eq. (1)**. It agree to

$$k(t, s) \approx \sum_{i,j=0}^N a_{i,j} \varphi_{i,j}(s) \varphi_{j,j}(t) = \Phi_J^T(s) A \Phi_J(t), \quad (23)$$

Where $A = (a_{i,j})_{0 \leq i,j \leq N}$. The next integral specified in (3.1) can be approximated as follows:

$$\begin{aligned} \int_0^1 k(t, s) v(s) ds &\approx \int_0^1 \varphi_J^T(s) A \varphi_J(t) (C^T \varphi_J(s)) ds. \\ &= C^T A \varphi_J(t) \int_0^1 \varphi_J^T(s) \varphi_J(s) ds = C^T A \varphi_J(t) \|\varphi_J\|^2, \end{aligned} \quad (24)$$

where

$$\|\varphi_J\| = \left(\int_0^1 \varphi_J^T(s) \varphi_J(s) ds \right)^{\frac{1}{2}}. \quad (25)$$

Now, for $t_j \leq t < t_{j+1}$, the Eq. (1) can be written in matrix form as follow:

$$C^T D_\varphi^j(t) = \mu_1 C^T \Psi(t) + \mu_2 C^T A(t) \|\varphi_J\|^2 + f(t), \quad 0 \leq t \leq 1. \quad (26)$$

4. Convergence

We are ready to formulate two theorems about errors in the approximation of u in the space V . Before that, recall that for $1 \leq q \leq \infty$, the space W_q^1 denotes Sobolev the space of functions whose weak first-order derivatives lie in the Lebesgue space L_q . In addition, let us set

$$\rho = \max\{t_{i+1} - t_i, \quad i = 0, 1, \dots, N-1\}. \quad (27)$$

Theorem 1. Ref. [9, 10] Let v^\sim be the finest approximation of $u \in W_\infty^1$ in space V with respect to the base L_∞ . Then,

$$\|v - v^\sim\|_\infty \leq M_1 \rho \|v'\|_\infty. \quad (28)$$

Where M_1 is constant.

Theorem 2. Ref. [9, 10] Let v^\sim exist the best approximation of $u \in W_\infty^2$ in space V with respect to the base L_∞ . Then,

$$\|v' - v^{\sim'}\|_{\infty} \leq M_2 p \|v''\|_{\infty} \quad (29)$$

where M_2 is a stable.

We are ready now, to formulate the convergence theorem for problem (1, 2).

Theorem .3 Let u be the exact solution of problem (1, 2) with v^{\sim} be the best estimate of u in the space V . The following conditions are satisfied:

- (a) $u \in W_{\infty}^1 \cap W_{\infty}^2$, (a) $u \in W_{\infty}^1 \cap W_{\infty}^2$,
- (b) $\frac{d^r v}{dt^r}$ for $r = 0, 1, 2$ are Limited functions,
- (c) $\frac{\partial k(t,s)}{\partial s}$ Dedicated to $(t, s) \in (0, 1) \times (0, 1)$.

Let E be the remaining error obtained by the solution of v^{\sim} . Then,

$$\lim_{j \rightarrow \infty} \|E(t)\|_{\infty} = 0. \quad (30)$$

Proof. Assume that for $0 \leq t \leq 1$,

$${}^c D_0^{\alpha(t)} v^{\sim}(t) = u_1 \int_0^t (t-s)^{-\beta} v^{\sim}(s) ds + u_2 \int_0^1 k^{\sim}(t,s) v^{\sim}(s) ds + f(t) + E_p(t), \quad (31)$$

where $E_p(t)$ show the remaining error. Then, from (1) and (31) we can write

$$\begin{aligned} E(t) &= {}^c D_0^{\alpha(t)} (v(t) - v^{\sim}(t)) \\ &= u_1 \int_0^t (t-s)^{-\beta} \left(v(s) - v^{\sim}(s) \right) ds - u_2 \int_0^1 (k(t,s)v(s) - k^{\sim}(t,s)v^{\sim}(s)) ds \\ &= {}^c D_0^{\alpha(t)} (v(t) - v^{\sim}(t)) - u_1 \int_0^t (t-s)^{-\beta} (v(s) - v^{\sim}(s)) ds \\ &= -u_2 \left(\int_0^1 k^{\sim}(t,s)(v(s) - v^{\sim}(s)) ds + \int_0^1 (k(t,s) - k^{\sim}(t,s)) v(s) ds \right). \end{aligned} \quad (32)$$

Then, taking into explanation of (32) and Theorem 1, we have

$$\|E\|_{\infty} \leq \|v^{\sim} - v^{\sim'}\|_{\infty} \max_{t \leq 0 \leq 1} \left(\int_0^t \frac{dx}{(t-x)^{\alpha}} + u_1 \|v - v^{\sim}\|_{\infty} \max_{0 \leq t \leq 1} \left(\int_0^t (t-s)^{-\beta} ds \right) + u_2 \|v - v^{\sim}\|_{\infty} \max_{0 \leq t \leq 1} \int_0^1 |k^{\sim}(t,s)| ds + \|u\|_{\infty} k_p \max_{0 \leq t \leq 1} \left\| \frac{\partial k(t,s)}{\partial s} \right\|_{\infty} \right). \quad (33)$$

where K is a constant. This gives

$$\|E\|_\infty \leq \frac{1}{1-\alpha} \|v^\sim - v^{\sim'}\|_\infty + \frac{u_1}{1-\beta} \|v^\sim - v^\sim\|_\infty + u_2 \left(\|v^\sim - v^\sim\|_\infty \|k^\sim(t,s)\|_\infty + k_p \|u\|_\infty \max_{0 \leq t \leq 1} \left\| \frac{\partial k(t,s)}{\partial s} \right\|_\infty \right). \tag{34}$$

Now, by Theorem.1 and Theorem .2, we have

$$\begin{aligned} \|E\|_\infty &\leq M_2 P \frac{1}{1-\alpha} \|v''\|_\infty + \frac{u_1}{1-\beta} M_1 p \|v'\|_\infty + u_2 \left(M_1 p \|v'\|_\infty \|k^\sim(t,s)\|_\infty + K_p \|u\|_\infty \max_{0 \leq t \leq 1} \left\| \frac{\partial k(t,s)}{\partial s} \right\|_\infty \right) \\ &= P \left[\frac{M_2}{1-\alpha} \|v''\|_\infty + \frac{M_1 u_1}{1-\beta} \|v'\|_\infty + u_2 M_1 \|v'\|_\infty \|k^\sim(t,s)\|_\infty + u_2 K \|u\|_\infty \max_{0 \leq t \leq 1} \left\| \frac{\partial k(t,s)}{\partial s} \right\|_\infty \right]. \end{aligned} \tag{35}$$

Now, given the limits for $k^\sim, \frac{\partial k(t,s)}{\partial s}$ and $\frac{d^r v}{d t^r}$ for $r = 0, 1, 2$,

it is clear that we have $\lim_{p \rightarrow 0} \|E_p(t)\|_\infty = 0$.

5. Numerical Experiments

In this segment, we present several test problems to demonstrate the accuracy and validity of the proposed method. All computational procedures are performed using Python. For each example, we use the following error rate to evaluate the accuracy of our results.

$$\|e\|_\infty = \|v - v^\sim\|_\infty.$$

Example 1. Let's consider the following variable-order fractional integro-differential equation that has a weak single kernel. (Ref. [8, 11]):

$${}^c D_0^{\alpha(t)} v(t) = \frac{1}{4} \int_0^t (t-s)^{-\beta} v(v) ds + \frac{1}{7} \int_0^1 \exp(t+s) v(s) ds + f(t), \quad 0 \leq t \leq 1$$

With the initial form $v(0) = 0$, For $\beta = \frac{1}{2}$ and the initial term f defined as

$$\begin{aligned} f(t) = & \frac{\Gamma(3) t^{-\alpha(t)+2}}{\Gamma(-\alpha(t)+3)} - \frac{\Gamma(2) t^{-\alpha(t)+1}}{\Gamma(-\alpha(t)+2)} - \frac{\sqrt{\pi} t^2 \sqrt{2\Gamma(3)}}{4\Gamma(\frac{7}{2})} - \frac{\sqrt{\pi} t \sqrt{2\Gamma(2)}}{4\Gamma(\frac{5}{2})} \\ & - \frac{\exp(1+t) - 3 \exp(t)}{7} \end{aligned}$$

The exact solution will be

$$v(t) = t^2 - t.$$

Figure.1 shows the absolute error for Example 1 with $\alpha \equiv 0.15$ and $J = 4, 5, 6, 7, 8$ on the knot vector

$$E = \{0, 0, 2^{-J}, 2 \times 2^{-J}, \dots, 2^{-1}, 2^{-1}, 2^{-1} + 2^{-J}, 2^{-1} + 2 \times 2^{-J}, \dots, 1, 1\}.$$

Here, we have repeated knots in $t = 0, \frac{1}{2}, 1$ and also the size of the coefficient matrix will be $2^J \times 2^J$. As we can see, the error increases as we approach the end of the interval $[0,1]$. The reason is that the equations of the system are written in terms of $t_j \leq t \leq t_{i+1}$ for $j = 0, 1, \dots, N$. On the other hand, the fractional term ${}^c D_0^{\alpha(t)} v(t)$ and the first term on the right-hand side of **Eq. (1)**, i.e.

$\int_0^t (t-s)^{-\beta} v(s) ds$ contain the integral from 0 to t . This shows that in the first part of the interval $[0,1]$ compared to the end of this interval there is more information about the solution. Therefore, we would expect to observe a smaller error in the first part $[0,1]$. Moreover, as we expected, the error decreases significantly as J increases.

Table 1 shows the absolute error in determining the coordinates, for example 1 with $J=7$ at $\alpha(t) = 0.15, \sin(t)$ and $\beta = 0.5, 0.7, 0.9$.

Example 2. Lets examine the following equation which is an equation of variable order.

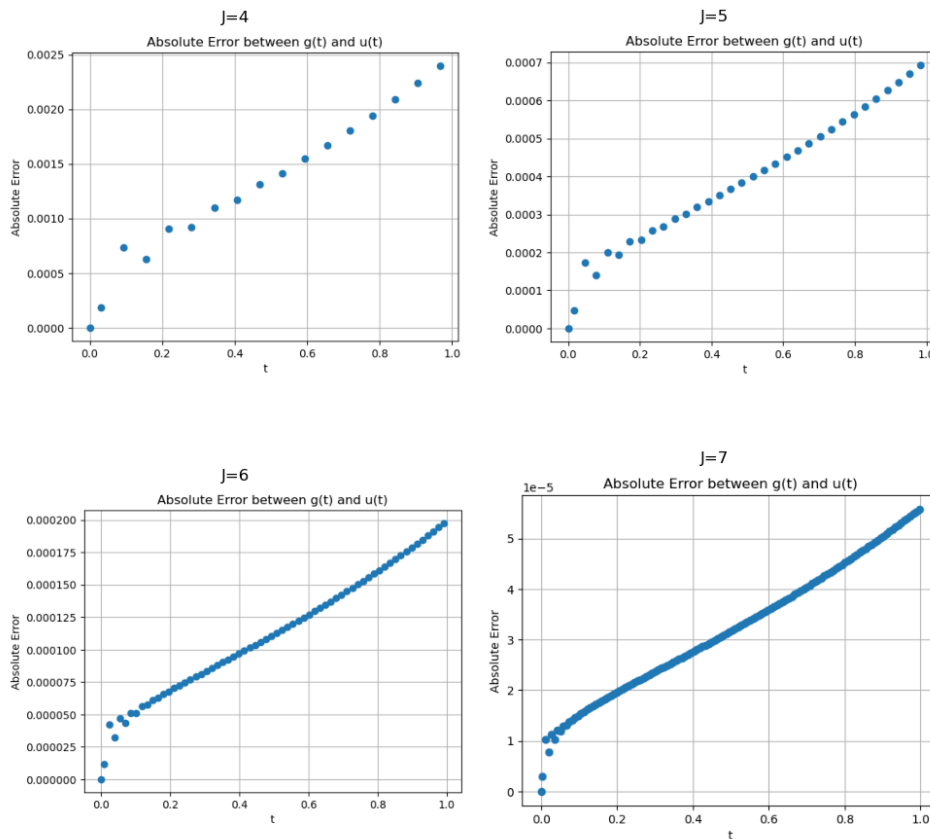


Figure 3. Estimations of the complete error for the solution of Example one with different values of J .

Fractional integro-differential equation characterized by a weakly singular kernel. (Ref. [8, 11]):

$${}^c D_0^{\alpha(t)} v(t) = 1/2 \int_0^t (t-s)^{-\beta} v(s) ds + 1/3 \int_0^1 (t-s) v(s) ds + f(t), \quad 0 \leq t \leq 1$$

With the initial condition $v(0) = 0$, used for $\beta = \frac{1}{2}$ and the initial term f defined as

$$f(t) = \frac{\Gamma(4)t^{-\alpha(t)+3}}{\Gamma(-\alpha(t)+4)} + \frac{\Gamma(3)t^{-\alpha(t)+2}}{\Gamma(-\alpha(t)+3)} - \frac{\sqrt{\pi} t^{\frac{5}{2}} \Gamma(4)}{\Gamma(\frac{7}{2})} - \frac{\sqrt{\pi} t^{\frac{7}{2}} \Gamma(4)}{2\Gamma(\frac{9}{2})} - \frac{7t}{36} + \frac{3}{20}$$

The require exact solution will determination in $v(t) = t^3 + t^2$.

Table 1. Absolute errors for example1 with $J = 7$ by different $\alpha(t)$ plus β

t	$\alpha(t) = 0.15$	$\alpha(t) = \sin t$	$\alpha(t) = \sin t$	$\alpha(t) = \sin t$
	$\beta = 0.5$	$\beta = 0.5$	$\beta = 0.7$	$\beta = 0.9$
1/6	1.3×10^{-5}	1.4×10^{-5}	1.5×10^{-5}	1.5×10^{-5}
1/3	2.4×10^{-5}	2.8×10^{-5}	2.6×10^{-5}	2.7×10^{-5}
1/2	3.1×10^{-5}	3.3×10^{-5}	3.4×10^{-5}	3.5×10^{-5}
2/3	3.7×10^{-5}	3.9×10^{-5}	4.1×10^{-5}	4.2×10^{-5}
5/6	4.7×10^{-5}	4.8×10^{-5}	4.9×10^{-5}	4.9×10^{-5}

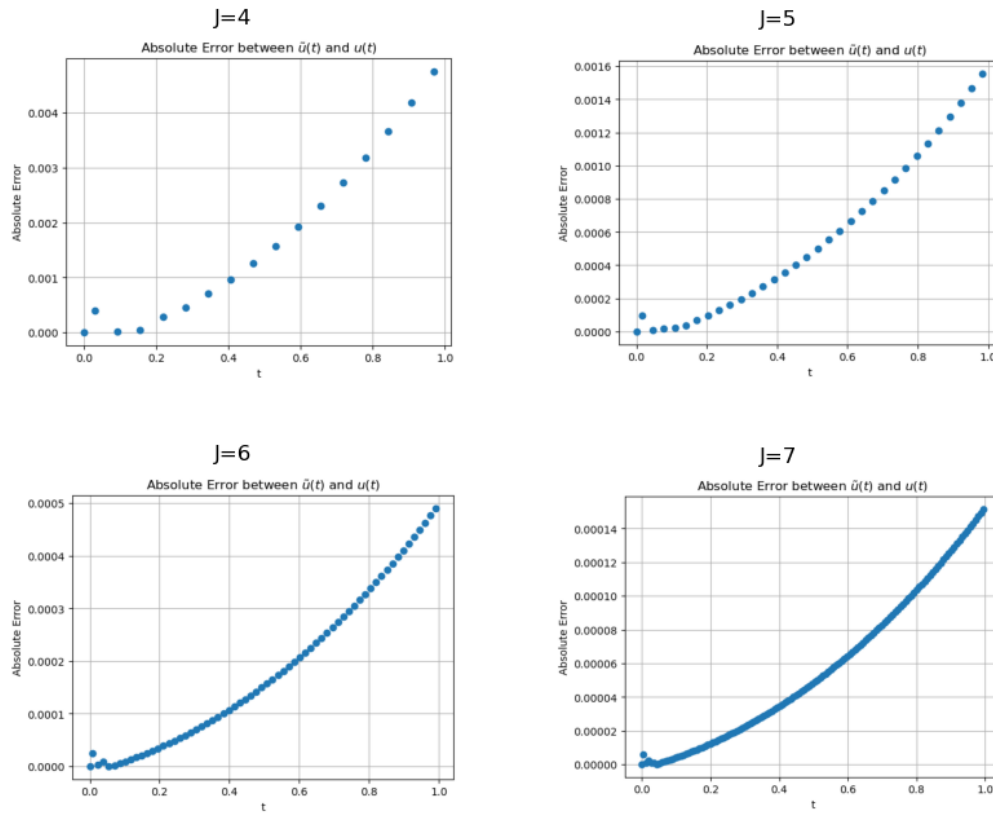


Figure 4. Calculation of complete error used for the solution of Example two through different values of J.

In Figure 2 shown the absolute error for example two with $\alpha \equiv 0.25$ and $J = 4,5,6,7,8$ on the knot vector.

$$E = \{0,0,2^{-J}, 2 \times 2^{-J}, \dots, 2^{-1}, 2^{-1}, 2^{-1} + 2^{-J}, 2^{-1} + 2 \times 2^{-J}, \dots, 1,1\}.$$

Here again we have a recurring knots on $t = 0, \frac{1}{2}, 1$. and the size of the coefficient matrix will be $2^J \times 2^J$. As we can see, as in Example.1, the error increases as we approach the end of the interval $[0,1]$. Moreover, as we expected, the error decreases as J increases.

Table 2. Show Absolute errors for Example two by $J = 7$ and $\beta = 0.5$ with different $\alpha (t)$

t	$\alpha (t) = 0.25$	$\alpha (t) = t$	$\alpha (t) = \sin t$	$\alpha (t) = \sin^2 t$
	$\beta = 0.5$	$\beta = 0.5$	$\beta = 0.5$	$\beta = 0.5$
1/6	1.3×10^{-5}	1.5×10^{-5}	1.7×10^{-5}	1.8×10^{-5}
1/3	2.1×10^{-5}	2.4×10^{-5}	2.6×10^{-5}	2.9×10^{-5}
1/2	5.0×10^{-5}	5.4×10^{-5}	5.7×10^{-5}	5.9×10^{-5}
2/3	6.4×10^{-5}	7.0×10^{-5}	7.3×10^{-5}	7.6×10^{-5}
5/6	1.1×10^{-4}	1.6×10^{-4}	1.8×10^{-4}	2.0×10^{-4}

Above table show the absolute error for example two with $J = 7$, and $\beta = 0.5$ for $\alpha(t) = 0.25, t, \sin(t)$ and $\sin^2 t$.

6. Conclusion

The proposed method for solving weakly single-kernel fractional integro-differential equations using multiple B-nodes is shown to be reliable and efficient. By analyzing the operational matrices and demonstrating the convergence of the approach, we have established a solid foundation for its application. The presented numerical examples confirm the accuracy and efficiency of the method, making it a promising solution for solving problems in this area. Future work can extend this approach to more complex problems and explore its potential in other areas of fractional calculus.

References

- [1] Mohammad, M., & Trounev, A. (2020). Fractional nonlinear Volterra–Fredholm integral equations involving Atangana–Baleanu fractional derivative: framelet applications. *Advances in Difference Equations*, 2020(1), 618.
- [2] Iserles, A. (2004). On the numerical quadrature of highly-oscillating integrals I: Fourier transforms. *IMA Journal of Numerical Analysis*, 24(3), 365-391.
- [3] Iserles, A. (2005). On the numerical quadrature of highly-oscillating integrals II: Irregular oscillators. *IMA journal of numerical analysis*, 25(1), 25-44.
- [4] Hieneman, M., Dunlap, G., & Kincaid, D. (2005). Positive support strategies for students with behavioral disorders in general education settings. *Psychology in the Schools*, 42(8), 779-794.
- [5] De Boor, C., & De Boor, C. (1978). *A practical guide to splines* (Vol. 27, p. 325). New York: Springer.
- [6] Dehestani, H., Ordokhani, Y., & Razzaghi, M. (2020). Numerical solution of variable-order time fractional weakly singular partial integro-differential equations with error estimation. *Mathematical Modelling and Analysis*, 25(4), 680-701.
- [7] Ghosh, B., & Mohapatra, J. (2023). Analysis of a second-order numerical scheme for time-fractional partial integro-differential equations with a weakly singular kernel. *Journal of Computational Science*, 74, 102157.
- [8] Keshavarz, E., & Ordokhani, Y. (2019). A fast numerical algorithm based on the Taylor wavelets for solving the fractional integro-differential equations with weakly singular kernels. *Mathematical Methods in the Applied Sciences*, 42(13), 4427-4443.
- [9] Lyche, T., Manni, C., & Speleers, H. (2017). B-splines and spline approximation. *Lecture notes*.
- [10] Kunoth, A., Lyche, T., Sangalli, G., Serra-Capizzano, S., Lyche, T., Manni, C., & Speleers, H. (2018). Foundations of spline theory: B-splines, spline approximation, and hierarchical refinement. *Splines and PDEs: From Approximation Theory to Numerical Linear Algebra: Cetraro, Italy 2017*, 1-76.
- [11] Mouley, J., & Mandal, B. N. (2021). Wavelet-based collocation technique for fractional integro-differential equation with weakly singular kernel. *Computational and Mathematical Methods*, 3(4), e1158.
- [12] Sadri, K., Hosseini, K., Baleanu, D., Ahmadian, A., & Salahshour, S. (2021). Bivariate Chebyshev polynomials of the fifth kind for variable-order time-fractional partial integro-differential equations with weakly singular kernel. *Advances in Difference Equations*, 2021, 1-26.
- [13] Schumaker, L. (2007). *Spline functions: basic theory*. Cambridge university press.
- [14] Taghipour, M., & Aminikhah, H. (2022). A difference scheme based on cubic B-spline quasi-interpolation for the solution of a fourth-order time-fractional partial integro-differential equation with a weakly singular kernel. *Sādhanā*, 47(4), 253.
- [15] Zhuang, P., Liu, F., Anh, V., & Turner, I. (2009). Numerical methods for the variable-order fractional advection-diffusion equation with a nonlinear source term. *SIAM Journal on Numerical Analysis*, 47(3), 1760-1781.